protein 2alpha and increases high-density lipoprotein biogenesis independent of alpha1-adrenoceptor blockade. *Circ Res.* 2007;101:156–165.
9. Arakawa R, Yokoyama S. Helical apolipoproteins stabilize ATP-binding cassette transporter A1 by protecting it from thiol protease-mediated degradation. *J Biol Chem.* 2002;277:22426–22429.
10. Arakawa R, Hayashi M, Remaley AT, Brewer BH Jr, Yamauchi Y, Yokoyama S. Phosphorylation and stabilization of ATP binding cassette transporter A1 by synthetic amphiphilic helical peptides. *J Biol Chem.* 2004;279:6217–6220.
11. Neufeld EB, Remaley AT, Demosky SJ, Stonik JA, Cooney AM, Comly M, Dwyer NK, Zhang M, Blanchette-Mackie J, Santamarina-Fojo S, Brewer HB Jr. Cellular localization and trafficking of the human ABCA1 transporter. *J Biol Chem.* 2001;276:27584–27590.
12. Neufeld EB, Stonik JA, Demosky SJ Jr, Knapper CL, Combs CA, Cooney A, Comly M, Dwyer N, Blanchette-Mackie J, Remaley AT, Santamarina-Fojo S, Brewer HB Jr. The ABCA1 transporter modulates late endocytic trafficking: insights from the correction of the genetic defect in Tangier disease. *J Biol Chem.* 2004;279:15571–15578.
13. Takahashi Y, Smith JD. Cholesterol efflux to apolipoprotein AI involves endocytosis and resecretion in a calcium-dependent pathway. *Proc Natl Acad Sci U S A.* 1999;96:11358–11363.
14. Chen W, Sun Y, Welch C, Gorelik A, Leventhal AR, Tabas I, Tall AR. Preferential ATP-binding cassette transporter A1-mediated cholesterol efflux from late endosomes/lysosomes. *J Biol Chem.* 2001;276:43564–43569.
15. Smith JD, Waelde C, Horwitz A, Zheng P. Evaluation of the role of phosphatidylserine translocase activity in ABCA1-mediated lipid efflux. *J Biol Chem.* 2002;277:17797–17803.
16. Hassan HH, Bailey D, Lee DY, Iatan I, Hafiane A, Ruel I, Krimbou L, Genest J. Quantitative analysis of ABCA1-dependent compartmentalization and trafficking of apolipoprotein A-I: Implications for determining cellular kinetics of nascent HDL biogenesis. *J Biol Chem.* 2008;283:11164–11175.
17. Munehira Y, Ohnishi T, Kawamoto S, Furuya A, Shitara K, Imamura M, Yokota T, Takeda S, Amachi T, Matsuo M, Kioka N, Ueda K. a1-syntrophin modulates turnover of ABCA1. *J Biol Chem.* 2004;279:15091–15095.
18. Okuhira K, Fitzgerald ML, Sarracino DA, Manning JJ, Bell SA, Goss JL, Freeman MW. Purification of ATP-binding cassette transporter A1 and associated binding proteins reveals the importance of beta1-syntrophin in cholesterol efflux. *J Biol Chem.* 2005;280:39653–39664.
19. Chen W, Wang N, Tall AR. A PEST deletion mutant of ABCA1 shows impaired identification and defective cholesterol efflux from late endosomes. *J Biol Chem.* 2005;280:29277–29281.
20. Witting SR, Maiorano JN, Davidson WS. Ceramide enhances cholesterol efflux to apolipoprotein A-I by increasing the cell surface presence of ATP-binding cassette transporter A1. *J Biol Chem.* 2003;278:40121–40127.
21. Faulkner LE, Panagotopulos SE, Johnson JD, Woollett LA, Hui DY, Witting SR, Maiorano JN, Davidson WS. An analysis of the role of a retroendocytosis pathway in ATP-binding cassette transporter (ABCA1)-mediated cholesterol efflux from macrophages. *J Lipid Res.* 2008;49:1322–1332.
22. Denis M, Landry YD, Aha X. ATP-binding cassette A1-mediated lipidation of apolipoprotein A-I occurs at the plasma membrane and not in the endocytotic compartment. *J Biol Chem.* 2008;283:16178–16186.
23. Arakawa R, Tamehiro N, Nishimaki-Mogami T, Ueda K, Yokoyama S. Fenofibric acid, an active form of fenofibrate, increases apolipoprotein A-I-mediated high-density lipoprotein biogenesis by enhancing transcription of ATP-binding cassette transporter A1 gene in a liver X receptor-dependent manner. *Arterioscler Thromb Vasc Biol.* 2005;25:1193–1197.
24. Yokoyama S, Tajima S, Yamamoto A. The process of dissolving apolipoprotein A-I in an aqueous buffer. *J Biochem (Tokyo).* 1982;91:1267–1272.
25. von Boxberg Y, Wütz R, Schwarz U. Use of the biotin-avidin system for labelling, isolation and characterization of neural cell-surface proteins. *Eur J Biochem.* 1990;190:249–256.
26. Vagin O, Turdikulova S, Yakubov I, Sachs G. Use of the H,K-ATPase beta subunit to identify multiple sorting pathways for plasma membrane delivery in polarized cells. *J Biol Chem.* 2005;280:14741–14754.
27. Abe-Dohmae S, Suzuki S, Wada Y, Aburatani H, Vance DE, Yokoyama S. Characterization of apolipoprotein-mediated HDL generation induced by cAMP in a murine macrophage cell line. *Biochemistry.* 2000;39:11092–11099.
28. Jackman MR, Shurety W, Ellis JA, Luzio JP. Inhibition of apical but not basolateral endocytosis of ricin and folate in Caco-2 cells by cytochalasin D. *J Cell Sci.* 1994;107:2547–2556.
29. Szaszi K, Paulsen A, Szabo EZ, Numata M, Grinstein S, Orlowski J. Clathrin-mediated endocytosis and recycling of the neuron-specific Na+/H+ exchanger NHE5 isoform. Regulation by phosphatidylinositol 3'-kinase and the actin cytoskeleton. *J Biol Chem.* 2002;277:42623–42632.
30. Hara H, Yokoyama S. Interaction of free apolipoproteins with macrophages. Formation of high density lipoprotein-like lipoproteins and reduction of cellular cholesterol. *J Biol Chem.* 1991;266:3080–3086.
31. Timmins JM, Lee JY, Boudyguina E, Kluckman KD, Brunham LR, Mulya A, Gebre AK, Coutinho JM, Colvin PL, Smith TL, Hayden MR, Maeda N, Parks JS. Targeted inactivation of hepatic Abca1 causes profound hypoalphalipoproteinemia and kidney hypercatabolism of apoA-I. *J Clin Invest.* 2005;115:1333–1342.
32. Nanjee MN, Cooke CJ, Olszewski WL, Miller NE. Lipid and apolipoprotein concentrations in prenodal leg lymph of fasted humans. Associations with plasma concentrations in normal subjects, lipoprotein lipase deficiency, and LCAT deficiency. *J Lipid Res.* 2000;41:1317–1327.

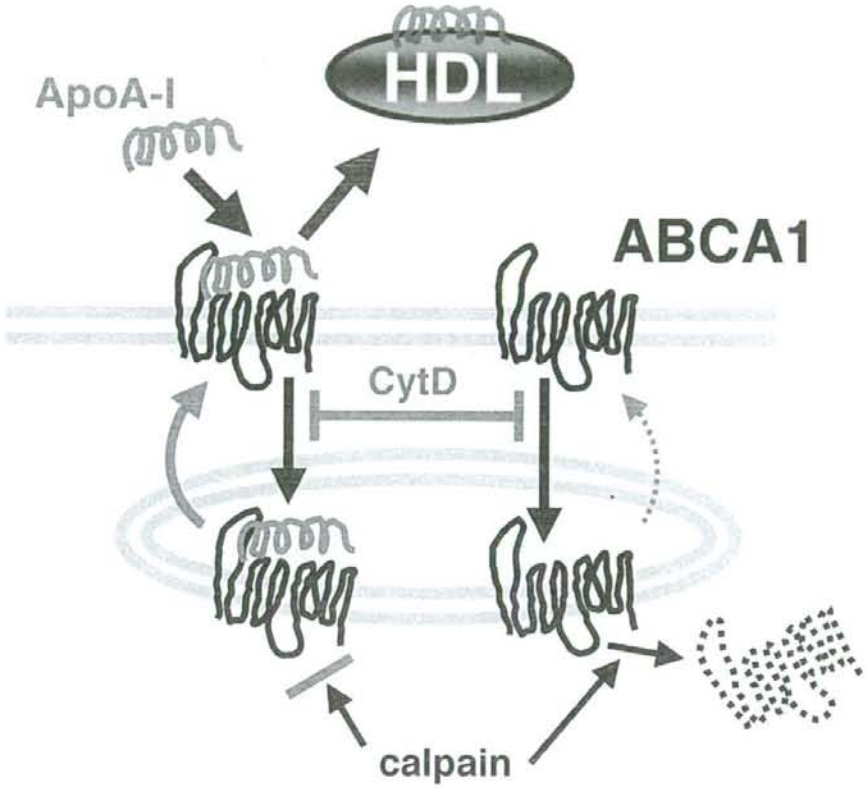

Supplementary Figure I. Schematic summary of the results. In the absence of apoA-I (right), ABCA1 is internalized and degraded by calpain and only very limited amount of ABCA1 could be recycled to the surface. Inhibition of calpain may lead to more recycle of ABCA1 to the surface. In the presence of apoA-I (left), ABCA1 is pre-protected by apoA-I in the surface against the intracellular calpain-mediated proteolysis. ABCA1 is therefore recycled to the surface. Inhibition of ABCA1 internalization by cytochalasin D (CytD) results in the increase of surface ABCA1. Surface ABCA1 is parallel to generation of HDL by apoA-I.

BIOCHEMICAL PHARMACOLOGY 76 (2008) 1006–1013

available at www.sciencedirect.com

ScienceDirect

journal homepage: www.elsevier.com/locate/biochempharm

The RXR agonists PA024 and HX630 have different abilities to activate LXR/RXR and to induce ABCA1 expression in macrophage cell lines

Tomoko Nishimaki-Mogami [a,*], *Norimasa Tamehiro* [a], *Yoji Sato* [a], *Kei-ichiro Okuhira* [a], *Kimie Sai* [a], *Hiroyuki Kagechika* [b], *Koichi Shudo* [d], *Sumiko Abe-Dohmae* [c], *Shinji Yokoyama* [c], *Yasuo Ohno* [a], *Kazuhide Inoue* [a,1], *Jun-ichi Sawada* [a]

[a] National Institute of Health Sciences, Tokyo, Japan
[b] School of Biomedical Science, Tokyo Medical and Dental University, Tokyo, Japan
[c] Nagoya City University Graduate School of Medical Sciences, Nagoya, Japan
[d] Itsu Research Institute, Tokyo, Japan

ARTICLE INFO

Article history:
Received 24 June 2008
Accepted 4 August 2008

Keywords:
Retinoid X receptor modulator
Peroxisome proliferator-activated receptor γ
Liver X receptor
ABCA1
HDL

ABSTRACT

Release of cellular cholesterol by ATP-binding cassette transporter (ABC)A1 and apolipoproteins is a major source of plasma high-density lipoprotein (HDL). Expression of ABC transporter A1 (ABCA1) is directly stimulated by liver X receptor (LXR)/retinoid X receptor (RXR) activation. We evaluated the abilities of two RXR agonists, PA024 and HX630, to increase ABCA1 expression. In differentiated THP-1 cells, the two agonists efficiently enhanced ABCA1 mRNA expression and apoA-I-dependent cellular cholesterol release. However, in RAW264 cells and undifferentiated THP-1 cells, PA024 was highly effective while HX630 was inactive in increasing ABCA1 mRNA. In parallel, the two agonists had different abilities to activate ABCA1 promoter in an LXR-responsive-element (LXRE)-dependent manner and to directly stimulate LXRα/RXR transactivation. The ability of HX630 to enhance ABCA1 expression was correlated closely with the cellular PPARγ mRNA level. Moreover, HX630 was able to activate PPARγ/RXR. Transfection of PPARγ in RAW264 cells induced HX630-mediated activation of LXRE-dependent transcription and ABCA1 promoter, suggesting the ability of HX630 to activate PPARγ-LXR-ABCA1 pathway. We conclude that RXR agonist PA024 and HX630 have different abilities to activate LXR/RXR, and that the cell-type-dependent effect of HX630 on ABCA1 expression and HDL generation is closely associated with this defect.

1. Introduction

ABC transporter A1 (ABCA1) mediates and rate-limits biogenesis of high-density lipoprotein (HDL) from helical apolipoprotein acceptors, such as apoA-I, and cellular cholesterol and phospholipids [1]. Mutations in the ABCA1 gene cause Tangier disease and other genetic HDL deficiencies [2–4]. Conversely, overexpression of ABCA1 in mice resulted in a mild elevation

* *Corresponding author at:* Division of Biosignaling, National Institute of Health Sciences, Kamiyoga 1-18-1, Setagaya-ku, Tokyo 158-8501, Japan. Tel.: +81 3 3700 9478; fax: +81 3 3707 6950.
E-mail address: mogami@nihs.go.jp (T. Nishimaki-Mogami).
[1] Present address: Department of Molecular and System Pharmacology, Graduate School of Pharmaceutical Sciences, Kyushu University, Fukuoka, Japan.
0006-2952/$ – see front matter
doi:10.1016/j.bcp.2008.08.005

of HDL cholesterol [5,6] and has been shown to protect animals from atherosclerosis [7,8]. Plasma HDL levels are inversely related to the risk of atherosclerotic cardiovascular disease [9], presumably because HDL functions to remove excess cholesterol from peripheral tissues and transport it to the liver for conversion to bile acids [10]. Accordingly, therapies that increase ABCA1 expression are a promising strategy for preventing and treating atherogenesis.

Cellular expression of ABCA1 is highly regulated. Loading cholesterol into macrophages and fibroblasts resulted in enhanced transcription of the ABCA1 gene by the reaction mediated by the oxysterol-activated liver X receptor (LXR) [11–14]. ABCA1 expression can also be increased by PPARα or PPARγ activators [15].

Retinoid X receptor (RXR) is a member of the nuclear receptor superfamily and forms heterodimers with a number of other receptors. RXR heterodimers, such as the peroxisome proliferator-activated receptor (PPAR)/RXR, LXR/RXR and the farnesoid X receptor (FXR)/RXR, can be activated by agonists for both RXR and the partner receptors and are classified as permissive heterodimers [16–18]. The thyroid hormone receptor/RXR or vitamin D receptor/RXR are not activated by RXR agonists and termed as non-permissive heterodimers [16–18]. A natural RXR agonist, 9-*cis*-retinoic acid, and synthetic RXR-selective ligands (rexinoids) have been shown to increase ABCA1 expression in macrophages [12,19,20].

In the present study, we evaluated the ability of two RXR agonists, PA024 and HX630, to induce ABCA1 expression in macrophage cell lines. Both PA024 and HX630 have been developed as RXR-selective agonists and are inactive alone in the HL-60 differentiation assay but strongly enhance the activity of low concentration of RAR-selective agonist AM80 [21]. However, their effects on the other RXR heterodimers are unknown. We found that PA024 potently induces ABCA1 expression in all cell models examined. However, HX630 failed to induce ABCA1 expression in RAW264 cells and undifferentiated THP-1 cells, and this defect was closely associated with the lack of ability to activate LXR/RXR. Instead, HX630 was able to activate PPARγ/RXR and induce ABCA1 expression in differentiated THP-1 cells. Our data also suggest the ability of HX630 to stimulate the PPARγ-LXR-ABCA1 pathway.

2. Materials and methods

2.1. Materials

22(R)-hydroxycholesterol and phorbol 12-myristate 13-acetate (PMA) was obtained from Sigma; troglitazone from BIOMOL Research Laboratories Inc. (Plymouth Meeting, PA, USA) HX630, PA024, and Am80 were prepared as described previously [21–23].

2.2. Cell culture and real time quantitative RT-PCRs

RAW264 cells were obtained from the Riken Gene Bank (Tsukuba, Japan) and maintained in Dulbecco's modified Eagle's medium (DMEM)/F-12 (1:1) containing 10% fetal calf serum. Cells were incubated for 24 h in serum-free medium containing 0.1% BSA in the presence or absence of 22(R)-hydroxycholesterol (2 μg/ml) and RXR agonists. THP-1 cells were maintained in RPMI 1640 medium containing 10% fetal calf serum. Cells were treated with RXR agonists in serum-free medium containing 0.2% BSA. Differentiation of THP-1 cells into macrophages was induced by treatment of the cells with 100 nM PMA for 48 h. RXR agonists were added to the medium during the last 24 h. Cells were harvested and total RNA was extracted using an RNeasy Mini Kit (Qiagen). The RNA samples were treated with DNase according to the manufacturer's protocol (Qiagen). Relative expression levels of mRNA were determined using a TaqMan one-step RT-PCR Master Mix Reagent Kit and an ABI Prism 7700 sequence detection system (Applied Biosystems). Primer/probe sequences used were as follows: human PPARγ forward primer, 5′-AGGCGAGGGCGATCTTG-3′, reverse primer, 5′-CCCATCAT-TAAGGAATTCATGTCAT-3′, probe, 5′FAM-CAGGAAAGACAA-CAGACAAATCACCATTCGT-TAMRA3′. The primer/probe sequences for mouse ABCA1 [24], human ABCA1, human ABCG1, and human LXRα [25] were the same as described previously. Expression data were normalized to 18S rRNA levels, and presented as the fold difference of treated cells against untreated cells.

2.3. Plasmid constructs

Plasmids for a LXRE-driven luciferase reporter and a PPAR response element (PPRE)-driven luciferase reporter (pPPRE-tk-Luc) and were constructed by inserting the cDNAs containing two copies of LXREa and LXREb from the sterol response element binding protein-1c promoter and two copies of PPRE from acyl-CoA oxidase, respectively, upstream from the thymidine kinase (tk) promoter. cDNAs encoding full-length human RXRα, LXRα, LXRβ, or PPARγ were PCR-cloned and inserted into mammalian expression vector pcDNA3.1 (Invitrogen). A mouse peripheral-type ABCA1 promoter (−1238/+57 of exon 1)-luciferase vector (pABCA1-Luc) has been described previously [24]. A mouse ABCA1 promoter construct containing mutation in LXRE (pABCA1:mutLXRE-Luc) was prepared as described previously [26].

2.4. Transient transfections and reporter gene assays

RAW264 cells were transfected with 1.0 μg of pABCA1-Luc or pABCA1:mutLXRE-Luc and 0.1 μg of Renilla luciferase vector (phRL-TK) (Promega) with SuperFect (Qiagen) in 24-well plates. For LXR activation studies, 1 μg of pLXRE-tk-Luc, 50 ng each of pcDNA3.1-LXR and pcDNA3.1-RXRα, and 0.7 μg of pSV-β-galactosidase control vector (Promega) were used. For the assay of PPARγ activation, cells were transfected with 1.3 μg of pPPRE-tk-Luc and 0.1 μg of Renilla luciferase vector (phRL-TK) (Promega) in the presence or absence of 50 ng each of pcDNA3.1-LXR and pcDNA3.1-RXRα. An empty pcDNA3.1 expression vector was used to maintain equal amounts of DNA for each transfection. Three hours after transfection, cells were exposed to RXR agonists in the medium containing 10% FCS for 24 h. Undifferentiated THP-1 cells were electroporatically transfected with 0. 4 μg of pABCA1-Luc or empty vector and 0.1 μg of phRL-TK using the Nucleofector transfection system (Amaxa Inc., Gaithersburg, MD) according to the manufacturer's protocol. Four hours after transfection, cells were exposed to RXR agonists in the medium containing 0.2%

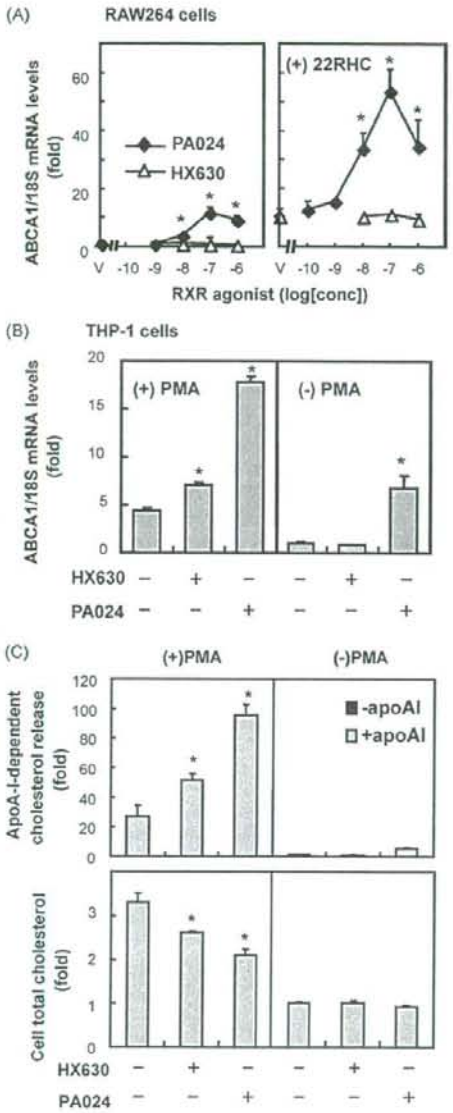

Fig. 1 – Effects of PA024 and HX630 on ABCA1 mRNA expression and cholesterol efflux in RAW264 cells, PMA-differentiated, and undifferentiated THP-1 cells. (A) RAW264 cells were treated for 24 h with PA024 or HX630 in the absence or presence of 22(R)-hydroxycholesterol (22RHC, 2 μg/ml). ABCA1 mRNA levels were measured with quantitative real-time RT-PCR analysis, standardized against 18S rRNA levels, and expressed as fold induction relative to the vehicle-treated cells (V, taken as 1). (B) PMA-differentiated or undifferentiated THP-1 cells were treated for 24 h with 100 nM PA024 or HX630. ABCA1 mRNA/18S rRNA levels were expressed as fold induction relative to the vehicle-treated undifferentiated cells. (C) PA024 and HX630 enhance apoA-I mediated cholesterol efflux and decrease the cellular cholesterol level in differentiated THP-1 cells. PMA-differentiated or undifferentiated THP-1 cells were treated for 24 h with 100 nM PA024 or HX630 in the presence or absence of apoA-I (15 μg/ml). ApoA-I-dependent release of cholesterol into the medium and cellular total cholesterol (2.69 ± 0.77 μg/mg protein and 15.31 ± 0.39 μg/mg protein, respectively, in control cells) were expressed as fold induction relative to the vehicle-treated undifferentiated cells. The values represent the average ± S.D. from three experiments. Significantly different from vehicle-treated cells (*).

FCS for 24 h. Luciferase and β-galactosidase activities were determined in cell lysates. Firefly luciferase activity was normalized to either that of Renilla luciferase or β-galactosidase for each well.

2.5. *Coactivator association assay using fluorescence polarization*

The assay was performed as described previously [27]. Briefly, TAMRA-labeled peptide (100 nM, with amino acid sequence ILRKLLQE) was incubated for 1 h with purified GST-fused human PPARγ LBD (1.5 μM) and ligands in 100 μl of buffer (10 mM Hepes, 150 mM NaCl, 2 mM $MgCl_2$, 5 mM DTT at pH 7.9) in a black polypropylene 96-well plate on a shaker. Ligand-dependent recruitment of the coactivator peptide was measured as increases in fluorescence polarization with a Fusionα-FP (PerkinElmer Life Science).

2.6. *Measurement of lipid efflux to apolipoprotein A-I (apoA-I)*

The differentiated or undifferentiated THP-1 cells were incubated in the presence or absence of 10 μg/ml of apoA-I in RPMI 1640 containing 0.2% BSA for 24 h. Lipid was extracted from the medium and the cells with chloroform/methanol (2:1, v/v) and hexane/isopropanol (3:2, v/v), respectively, and cholesterol and choline-phospholipid were determined by enzymatic methods specific for each lipid [28].

2.7. *Statistical analysis*

Data were analyzed by ANOVA followed by the Student–Newman–Keuls method. Statistical significance was established at the $P < 0.05$ level.

3. Results

3.1. *RXR agonist PA024 and HX630 show different abilities to induce ABCA1 expression*

We tested the ability of RXR agonist PA024 and HX630 to induce ABCA1 expression in murine macrophage-like cell line, RAW264. Treatment of RAW264 cells with PA024 markedly induced ABCA1 mRNA expression, which peaked at 100 nM, whereas HX630 up to 1 μM had no effect (Fig. 1A left). Expression of ABCA1 can be stimulated by oxysterol-activated

LXR [11,13,14]. The addition of 22(R)-hydroxycholesterol to the medium increased ABCA1 expression and strongly enhanced the effect of PA024 (Fig. 1A right). This combination had a greater than additive effect, whereas HX630 again had no effect.

The effect of two RXR agonists on ABCA1 expression was also studied in a human monocytic leukemia cell line, THP-1 (Fig. 1B). PA024 (100 nM) increased the ABCA1 mRNA level both in PMA-differentiated and undifferentiated cells (by 4- and 7-fold, respectively). In contrast, HX630 (100 nM) did not affect the ABCA1 mRNA level in undifferentiated cells. However, the same concentration of HX630 did raise the ABCA1 mRNA level in PMA-differentiated cells by 1.6-fold.

ABCA1 has been shown to play a critical role in the assembly of HDL from apoA-I and cellular cholesterol and phospholipids. We examined the effect of the two RXR agonists on apoA-I-mediated cholesterol release (HDL production) in THP-1 cells (Fig. 1C). HX630 and PA024 at 100 nM increased the amount of cholesterol released into the medium in the presence of apoA-I (by 2- and 3.4-fold, respectively) in differentiated cells, and this increase was accompanied by a decrease in the cellular total cholesterol level. In contrast, the same concentration of HX630 had no effect in undifferentiated cells.

3.2. *PA024 but not HX630 activates LXR/RXR and ABCA1 promoter*

To determine whether the different abilities of the two RXR agonists in ABCA1 mRNA induction were resulted from different abilities in ABCA1 gene transcription, we examined their effects on ABCA1 promoter activity. An ABCA1 promoter (−1238/+57 of exon 1)-luciferase construct was transfected into RAW264 cells. As shown in Fig. 2A, PA024 markedly increased the ABCA1 promoter transcription, and the increase caused by PA024 was lost when a mutation was introduced into LXRE in the promoter. In contrast, HX630 up to 1 μM had no effect on the promoter activity. Similarly, when the ABCA1 promoter was transfected into undifferentiated THP-1 cells, PA024 augmented the promoter activity in an LXRE-dependent manner, but HX630 had no effect (Fig. 2B). These findings indicate that PA024-induced activation of ABCA1 promoter was mediated by LXRE. We intended to examine the promoter activity in PMA-differentiated THP-1 cells. However, transfection of the plasmid into the differentiated THP-1 cells was unsuccessful. In addition, cells harboring transfected DNA did not undergo differentiation with PMA.

The possibility that PA024 but not HX630 activates LXR/RXR was tested using a reporter assay. Transfection of the LXRE-driven luciferase-reporter vector alone into RAW264 cells yielded substantial luciferase activity, indicating transcriptional activation by endogenous receptor(s), and this endogenous LXRs-mediated activity was increased by PA024, but not HX630 (Fig. 3 left). Co-transfection of LXRα and RXRα expression vectors enhanced the effect of PA024, whereas HX630 again had no effect (Fig. 3 middle). Expressions of LXRβ and RXRα augmented luciferase transcription in the vehicle-treated control (Fig. 3 right). However, the response elicited by PA024 was small and similar to that in cells without LXR/RXR plasmids (Fig. 3 left). HX630 again had no effect.

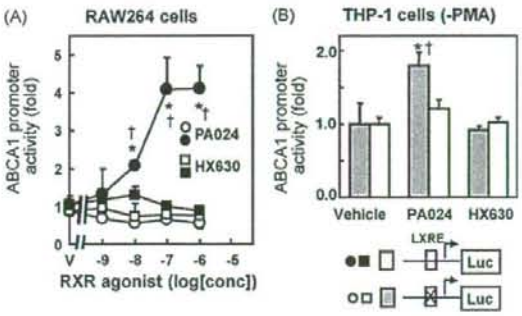

Fig. 2 – PA024 but not HX630 augments ABCA1 promoter activity in RAW264 cells (A) and undifferentiated THP-1 cells (B). Cells were transfected with a pABCA1-Luc (closed symbols) or pABCA1:mutLXRE-Luc (open symbols) reporter plasmid together with a phRL-TK internal control as described in Section 2.4, and treated with indicated concentrations (for A) or 100 nM (for B) of PA024 and HX630. Luciferase activity in the cell extract was normalized using Renilla luciferase activity and expressed as fold induction relative to vehicle-treated cells (indicated as V). The data represent the average ± S.D. of three experiments. Significantly different from vehicle-treated cells (*) or LXRE-mutated promoter (†).

3.3. *HX630 and PA024 activate PPARγ/RXR*

The ability of HX630 and PA024 to activate PPARγ/RXR was tested in RAW264 cells transfected with a PPRE-driven luciferase-reporter vector (Fig. 4A). When PPARγ/RXR was transfected into the cells, the two agonists markedly increased luciferase activity. RXR-homodimer has been shown to activate transcription of the DR-1 element [29]. Upon transfection of

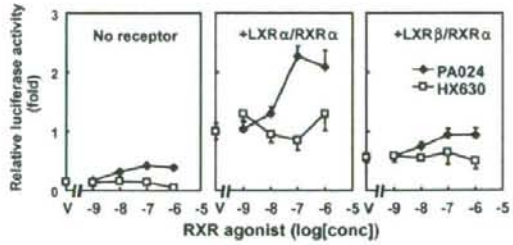

Fig. 3 – PA024 but not HX630 augments LXRα/RXR transactivation. RAW264 cells were transfected with LXREx4-tk-Luc reporter plasmid together with a β-gal internal control in the absence (A) or presence of expression plasmids for human LXRα and RXRα (B) or LXRβ and RXRα (C). The cells were treated with the indicated concentrations of PA024 or HX630. Luciferase activity in the cell extract was normalized using β-gal and expressed as fold induction relative to vehicle-treated cells (indicated as V). The data represent the average ± S.D. of three incubations.

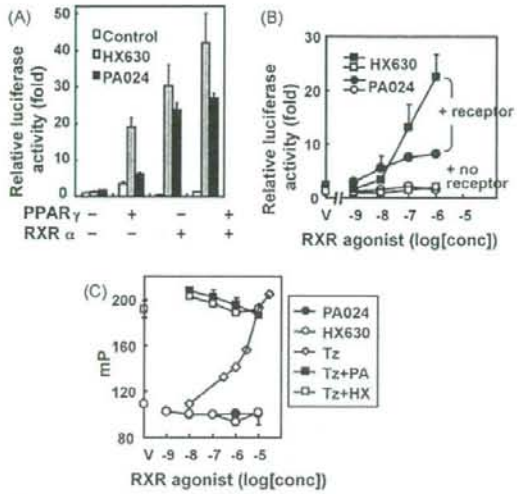

Fig. 4 – PA024 and HX630 stimulate PPARγ/RXR transactivation. (A) RAW264 cells were transfected with a PPRE-tk-Luc reporter plasmid together with a phRL-TK internal control in the presence or absence of expression plasmids for human PPARγ and RXRα. The cells were treated with 100 nM PA024 or HX630 for 24 h before analysis. (B) Dose–response of RXR agonists for activation of a reporter gene by PPARγ/RXR. Cells were transfected with a PPRE-tk-Luc reporter plasmid in the absence (open symbols) or presence (closed symbols) of the PPARγ expression plasmid and treated with drugs for 24 h. Luciferase activity stimulated by PPARγ and endogenous RXR in the cell extract was determined, normalized, and expressed as fold induction relative to vehicle-treated cells without exogenous receptor expression. The values represent the average ± S.D. of three incubations. (C) RXR agonists do not affect binding of troglitazone to PPARγ. A fluorescent-tagged SRC-1 peptide (0.1 μM) was incubated with 1.5 μM PPARγ ligand binding domain in the presence of various concentrations of PA024 and HX630 in the presence or absence of 10 μM troglitazone (Tz). Ligand-induced association of coactivator peptide with the receptor was monitored by increases in millipolarization fluorescence units (mP).

RXRα alone, the two agonists increased luciferase activity, indicating substantial activation of RXRα homodimer. However, when PPARγ alone was co-transfected, both agonists greatly enhanced transcription, suggesting that they have abilities to activate PPARγ/RXR heterodimer made from exogenous PPARγ and endogenous RXR. In this reporter assay system using exogenous PPARγ and endogenous RXR, HX630 activated PPARγ/RXR-dependent transcription more potently than PA024 at concentrations higher than 100 nM (Fig. 4B). To exclude the possibility that the HX630 and PA024 bind to PPARγ as a ligand, coactivator-association assay was performed. As shown in Fig. 4C, neither HX630 nor PA024 induced an interaction between fluorescence-labeled coactivator peptide and the PPARγ ligand binding domain *in vitro*, while the PPARγ agonist troglitazone strongly induced association. Furthermore, these RXR agonists did not affect the PPARγ-coactivator interaction elicited by 10 μM troglitazone. These findings indicate that the two RXR agonists were able to activate PPARγ/RXR.

3.4. *Possible stimulation of PPARγ-LXR-ABCA1 pathway by HX630*

LXRα gene is known to be a direct target of PPARγ/RXR, and stimulation of PPARγ has been shown to increase LXR-target gene expression by increasing LXRα expression [30]. We therefore examined the ability of HX630 to enhance LXR-target gene transcription by activating PPARγ/RXR. LXRE-driven luciferase assay was performed in RAW264 cells with or without co-transfection of PPARγ. As shown in Fig. 5A, HX630 augmented luciferase transcription in the presence but not in the absence or PPARγ. This effect was enhanced by increasing the amount of the PPARγ expression plasmid and the combination of HX630 and the LXR agonist 22(R)-hydroxycholesterol had an additive effect. The activity of ABCA1 promoter was also increased by HX630 when PPARγ was co-transfected (Fig. 5B)

The level of PPARγ mRNA was very low in undifferentiated THP-1 cells (not treated with PMA) but up-regulated during differentiation with PMA (Fig. 6). The levels of PPARγ-target gene CD36 and LXRα mRNA were unaffected by HX630 (100 nM) in undifferentiated cells but increased in PMA-differentiated cells (by 1.4- and 1.6-fold, respectively). In parallel with these changes, LXRα-target ABCG1 expression was unaffected by HX630 in undifferentiated THP-1 cells but increased in differentiated cells (by 3.9-fold). PA024 (100 nM) effectively raised ABCG1 and LXRα levels in undifferentiated

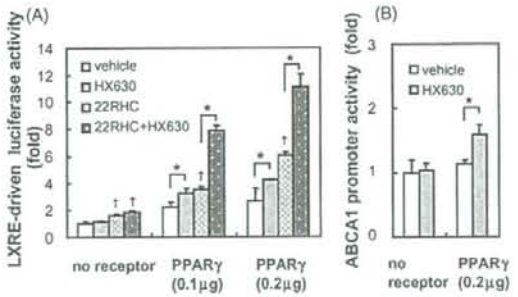

Fig. 5 – HX630 activates LXRE-driven luciferase (A) or ABCA1 promoter (B) gene transcription upon co-expression of PPARγ. RAW264 cells were transfected with an LXREx4-tk-Luc or a pABCA1-Luc reporter plasmid and a phRL-TK internal control in the presence of 0–0.2 μg of PPARγ plasmid and treated for 24 with 100 nM HX630 in the presence or absence of 0.5 μg/ml 22(R)-hydroxycholesterol (22RHC). Luciferase activity in the cell extract was determined and normalized. The values represent the average ± S.D. of three experiments. Significantly different from respective control (*) or vehicle-treated cells (†).

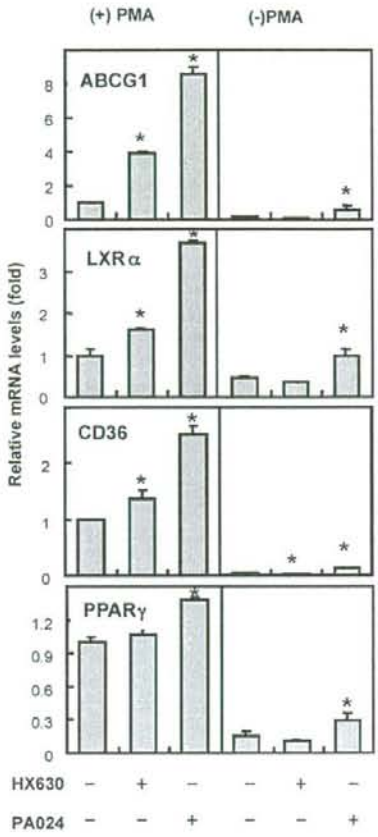

Fig. 6 – PA024 and HX630 increase LXR- and PPARγ-target gene expressions in PMA-differentiated THP-1 cells. PMA-differentiated or undifferentiated THP-1 cells were treated for 24 h with 100 nM PA024 or HX630. The expressions of ABCG1, PPARγ, and LXRα mRNA were measured as described in the legend to Fig. 1B. The values represent the average ± S.D. relative to the PMA-treated control cells (taken as 1) from three experiments. * Significantly different from vehicle-treated cells.

cells, and the effect was drastically increased in PMA-differentiated cells.

4. Discussion

In the present study, we found that RXR agonist PA024 efficiently enhanced ABCA1 mRNA expression in all cell lines tested and strongly promoted apoA-I-mediated cholesterol release (HDL generation) from PMA-differentiated THP-1 cells (Fig. 1B and C). However, HX630 was unable to raise the ABCA1 mRNA level in RAW264 cells (Fig. 1A) and undifferentiated THP-1 cells (Fig. 1B), but was active in differentiated THP-1 cells (Fig. 1B).

The different abilities of the two agonists to induce ABCA1 mRNA expression in RAW264 cells and undifferentiated THP-1 cells were paralleled with their different abilities to activate ABCA1 promoter (Fig. 2). PA024 increased the ABCA1 promoter activity in an LXRE-dependent manner, suggesting that the effect of PA024 was primarily mediated by LXR/RXR activation. Indeed, PA024 strongly stimulated LXRα/RXR-dependent transcription in a cellular transactivation assay (Fig. 3). In contrast, HX630 failed to stimulate the ABCA1 promoter activity. Because HX630 had no capability to directly activate LXR/RXR, suggesting that the failure of ABCA1 induction by HX630 is attributable to this defect.

However, HX630 was able to increase ABCA1 mRNA expression and promote apoA-I-mediated cholesterol release (HDL generation) in PMA-differentiated THP-1 cells (Fig. 1B and C). HX630 was able to induce another LXR-target gene ABCG1 mRNA expression in differentiated cells but not in undifferentiated cells (Fig. 6). These findings suggest that HX630 might increase LXR-target gene transcription in differentiated THP-1 cells.

The LXRα gene is known to be a direct target of PPARγ, and stimulation of PPARγ by agonists has been shown to increase ABCA1 expression by raising LXRα level [30]. We showed that both HX630 and PA024 were able to activate PPARγ/RXR in a cellular transactivation assay (Fig. 4). Furthermore, if PPARγ-expression plasmid was co-transfected into RAW264 cells, HX630 was able to stimulate an LXRE-dependent reporter gene transcription and the ABCA1 promoter activity, as well (Fig. 5). These findings suggest the ability of HX630 to stimulate the PPARγ-LXR-ABCA1 pathway. The level of PPARγ mRNA was greatly induced by differentiation of THP-1 cells with PMA (Fig. 6). In addition, the differentiation augmented HX630-mediated expression of LXR-target ABCA1 and ABCG1 and PPARγ-target LXRα and CD36. Both endogenous PPARγ activity (Fig. 4A and B) and HX630-induced ABCA1 expression (Fig. 1A) were undetectable in RAW264 cells. These findings indicate a close correlation between the ability of HX630 to enhance LXR-target gene expression and the cellular PPARγ mRNA level. The activation of PPARγ/RXR by HX630 primary may elevate LXRα and thereby enhances ABCA1 expression in PMA-differentiated THP-1 cells. Possibility remains that HX630 stimulates LXR/RXR in this cell model. However, we were unable to investigate this possibility due to very low efficiency in DNA transfection in PMA-differentiated cells. Another possibility is that activation of RXR heterodimer(s) other than PPARγ/RXR may also be responsible for the HX630-mediated ABCA1 expression in this cell line. A study has shown that RAR activators increase ABCA1 expression in mouse peripheral macrophages, and that RAR/RXR stimulated the ABCA1 promoter activity via the same DR4 element as LXR/RXR [31]. However, when PMA-differentiated THP-1 cells were treated with RAR agonist AM80 [21], the ABCA1 mRNA level was unchanged (data not shown), suggesting that the RAR/RXR-mediated promoter activation may not make a large contribution to ABCA1 expression in this cell line.

Inductions of ABCA1 and HDL generation by PA024 and HX630 were accompanied by a decrease in the cellular cholesterol level (Fig. 1C). In particular, our findings show the effectiveness of direct activation of LXR/RXR by PA024 (Fig. 3). Although LXR/RXR is known to be permissive in terms

of RXR agonist activation [16,17], HX630 was unable to activate LXR/RXR (Fig. 3). Administration of RXR agonists to mice leads to increases in HDL cholesterol levels [20]. RXR modulators are promising therapeutic strategies [32]. However, increases in serum triglyceride due to RXR agonists are postulated to occur via activation of LXR/RXR, leading to enhanced lipogenesis in response to induction of hepatic SREBP-1c expression [33]. Heterodimer-selective RXR agonists without the ability to directly activate LXR/RXR, may be a promising target for the development of drugs without adverse effects. Synthetic RXR agonists that retain the ability to activate PPARγ/RXR, but have less effect on LXR/RXR and RAR/RXR, have been reported, and pharmacological advantages of these heterodimer-selective RXR agonists as anti-diabetes agents have been demonstrated [34]. The molecular basis of such heterodimer selectivity has not fully been clarified. The mechanism underlying HX630 heterodimer selectivity awaits further investigation.

Acknowledgments

This work was supported in part by a grant from the Japan Health Sciences Foundation, a grant (MF-16) from the Organization for Pharmaceutical Safety and Research, and Grant-in-Aid for Scientific Research 20590116 from Japan Society for the Promotion of Science.

REFERENCES

[1] Yokoyama S. Assembly of high-density lipoprotein. Arterioscler Thromb Vasc Biol 2006;26:20–7.
[2] Bodzioch M, Orso E, Klucken J, Langmann T, Bottcher A, Diederich W, et al. The gene encoding ATP-binding cassette transporter 1 is mutated in Tangier disease. Nat Genet 1999;22:347–51.
[3] Brooks-Wilson A, Marcil M, Clee SM, Zhang LH, Roomp K, van Dam M, et al. Mutations in ABC1 in Tangier disease and familial high-density lipoprotein deficiency. Nat Genet 1999;22:336–45.
[4] Rust S, Rosier M, Funke H, Real J, Amoura Z, Piette JC, et al. Tangier disease is caused by mutations in the gene encoding ATP-binding cassette transporter 1. Nat Genet 1999;22:352–5.
[5] Singaraja RR, Bocher V, James ER, Clee SM, Zhang LH, Leavitt BR, et al. Human ABCA1 BAC transgenic mice show increased high density lipoprotein cholesterol and apoAI-dependent efflux stimulated by an internal promoter containing liver X receptor response elements in intron 1. J Biol Chem 2001;276:33969–7.
[6] Vaisman BL, Lambert G, Amar M, Joyce C, Ito T, Shamburek RD, et al. ABCA1 overexpression leads to hyperalphalipoproteinemia and increased biliary cholesterol excretion in transgenic mice. J Clin Invest 2001;108:303–9.
[7] Joyce CW, Amar MJ, Lambert G, Vaisman BL, Paigen B, Najib-Fruchart J, et al. The ATP binding cassette transporter A1 (ABCA1) modulates the development of aortic atherosclerosis in C57BL/6 and apoE-knockout mice. Proc Natl Acad Sci USA 2002;99:407–12.
[8] Singaraja RR, Fievet C, Castro G, James ER, Hennuyer N, Clee SM, et al. Increased ABCA1 activity protects against atherosclerosis. J Clin Invest 2002;110:35–42.
[9] Gordon T, Castelli WP, Hjortland MC, Kannel WB, Dawber TR. High density lipoprotein as a protective factor against coronary heart disease. The Framingham study. Am J Med 1977;62:707–14.
[10] Fielding CJ, Fielding PE. Molecular physiology of reverse cholesterol transport. J Lipid Res 1995;36:211–28.
[11] Costet P, Luo Y, Wang N, Tall AR. Sterol-dependent transactivation of the ABC1 promoter by the liver X receptor/retinoid X receptor. J Biol Chem 2000;275:28240–5.
[12] Langmann T, Klucken J, Reil M, Liebisch G, Luciani MF, Chimini G, et al. Molecular cloning of the human ATP-binding cassette transporter 1 (hABC1): evidence for sterol-dependent regulation in macrophages. Biochem Biophys Res Commun 1999;257:29–33.
[13] Schwartz K, Lawn RM, Wade DP. ABC1 gene expression and apoA-I-mediated cholesterol efflux are regulated by LXR. Biochem Biophys Res Commun 2000;274:794–802.
[14] Venkateswaran A, Laffitte BA, Joseph SB, Mak PA, Wilpitz DC, Edwards PA, et al. Control of cellular cholesterol efflux by the nuclear oxysterol receptor LXR alpha. Proc Natl Acad Sci USA 2000;97:12097–102.
[15] Chinetti G, Lestavel S, Bocher V, Remaley AT, Neve B, Torra IP, et al. PPAR-alpha and PPAR-gamma activators induce cholesterol removal from human macrophage foam cells through stimulation of the ABCA1 pathway. Nat Med 2001;7:53–8.
[16] Chawla A, Repa JJ, Evans RM, Mangelsdorf DJ. Nuclear receptors and lipid physiology: opening the X-files. Science 2001;294:1866–70.
[17] Mangelsdorf DJ, Evans RM. The RXR heterodimers and orphan receptors. Cell 1995;83:841–50.
[18] Mukherjee R, Davies PJ, Crombie DL, Bischoff ED, Cesario RM, Jow L, et al. Sensitization of diabetic and obese mice to insulin by retinoid X receptor agonists. Nature 1997;386:407–10.
[19] Claudel T, Leibowitz MD, Fievet C, Tailleux A, Wagner B, Repa JJ, et al. Reduction of atherosclerosis in apolipoprotein E knockout mice by activation of the retinoid X receptor. Proc Natl Acad Sci USA 2001;98:2610–5.
[20] Repa JJ, Turley SD, Lobaccaro JA, Medina J, Li L, Lustig K, et al. Regulation of absorption and ABC1-mediated efflux of cholesterol by RXR heterodimers. Science 2000;289:1524–9.
[21] Kagechika H, Shudo K. Synthetic retinoids: recent developments concerning structure and clinical utility. J Med Chem 2005;48:5875–83.
[22] Ohta K, Kawachi E, Inoue N, Fukasawa H, Hashimoto Y, Itai A, et al. Retinoidal pyrimidinecarboxylic acids. Unexpected diaza-substituent effects in retinobenzoic acids. Chem Pharm Bull (Tokyo) 2000;48:1504–13.
[23] Umemiya H, Fukasawa H, Ebisawa M, Eyrolles L, Kawachi E, Eisenmann G, et al. Regulation of retinoidal actions by diazepinylbenzoic acids. Retinoid synergists which activate the RXR–RAR heterodimers. J Med Chem 1997;40:4222–34.
[24] Suzuki S, Nishimaki-Mogami T, Tamehiro N, Inoue K, Arakawa R, Abe-Dohmae S, et al. Verapamil increases the apolipoprotein-mediated release of cellular cholesterol by induction of ABCA1 expression via Liver X receptor-independent mechanism. Arterioscler Thromb Vasc Biol 2004;24:519–25.
[25] Fu X, Menke JG, Chen Y, Zhou G, MacNaul KL, Wright SD, et al. 27-hydroxycholesterol is an endogenous ligand for liver X receptor in cholesterol-loaded cells. J Biol Chem 2001;276:38378–87.
[26] Tamehiro N, Shigemoto-Mogami Y, Kakeya T, Okuhira K, Suzuki K, Sato R, et al. Sterol regulatory element-binding protein-2- and liver X receptor-driven dual promoter regulation of hepatic ABC transporter A1 gene expression: mechanism underlying the unique response to cellular cholesterol status. J Biol Chem 2007;282:21090–9.

[27] Nishimaki-Mogami T, Une M, Fujino T, Sato Y, Tamehiro N, Kawahara Y, et al. Identification of intermediates in the bile acid synthetic pathway as ligands for the farnesoid X receptor. J Lipid Res 2004;45: 1538–45.
[28] Abe-Dohmae S, Suzuki S, Wada Y, Aburatani H, Vance DE, Yokoyama S. Characterization of apolipoprotein-mediated HDL generation induced by cAMP in a murine macrophage cell line. Biochemistry 2000;39:11092–9.
[29] Umemiya H, Kagechika H, Fukasawa H, Kawachi E, Ebisawa M, Hashimoto Y, et al. Action mechanism of retinoid-synergistic dibenzodiazepines. Biochem Biophys Res Commun 1997;233:121–5.
[30] Chawla A, Boisvert WA, Lee CH, Laffitte BA, Barak Y, Joseph SB, et al. A PPAR gamma-LXR-ABCA1 pathway in macrophages is involved in cholesterol efflux and atherogenesis. Mol Cell 2001;7:161–71.
[31] Costet P, Lalanne F, Gerbod-Giannone MC, Molina JR, Fu X, Lund EG, et al. Retinoic acid receptor-mediated induction of ABCA1 in macrophages. Mol Cell Biol 2003;23:7756–66.
[32] Altucci L, Leibowitz MD, Ogilvie KM, de Lera AR, Gronemeyer H. RAR and RXR modulation in cancer and metabolic disease. Nat Rev Drug Discov 2007;6:793–810.
[33] Schultz JR, Tu H, Luk A, Repa JJ, Medina JC, Li L, et al. Role of LXRs in control of lipogenesis. Genes Dev 2000;14:2831–8.
[34] Michellys PY, Ardecky RJ, Chen JH, Crombie DL, Etgen GJ, Faul MM, et al. Novel (2E,4E,6Z)-7-(2-alkoxy-3,5-dialkylbenzene)-3-methylocta-2,4,6-trienoic acid retinoid X receptor modulators are active in models of type 2 diabetes. J Med Chem 2003;46:2683–96.

Circ J 2008; **72:** 1569–1575

Practical Risk Prediction Tools for Coronary Heart Disease in Mild to Moderate Hypercholesterolemia in Japan

— Originated From the MEGA Study Data —

Tamio Teramoto, MD; Yasuo Ohashi, PhD*; Noriaki Nakaya, MD**; Shinji Yokoyama, MD†; Kyoichi Mizuno, MD††; Haruo Nakamura, MD‡ for the MEGA Study Group

Background A simple and practical risk prediction tool for coronary heart disease (CHD) to determine the specific risk level in each patient that fits the true clinical practice setting is needed and would be valuable in Japan.

Methods and Results A 5-year risk prediction score and chart for CHD based on the MEGA study data was developed in the present study. The MEGA risk prediction score and chart were constructed based on the coefficient of each risk factor. The risk factors included in these risk prediction tools were: treatment (diet, diet plus pravastatin), sex, age, baseline high-density lipoprotein-cholesterol, baseline low-density lipoprotein-cholesterol, glucose abnormality (diabetes and impaired fasting glucose), hypertension, and smoking. The MEGA risk prediction score comprised the risk score for each risk factor, and it can predict 5-year risk for CHD with 5 levels of risk, based on the total risk score. The MEGA risk prediction chart more accurately predicts risk, by reflecting the accumulation of risk factors and using an 8-color visual chart.

Conclusions The MEGA risk prediction score and chart, developed from the MEGA study data, more easily and accurately assesses the 5-year CHD risk in mild to moderate hypercholesterolemic patients in the usual clinical practice setting in Japan. (*Circ J* 2008; **72:** 1569–1575)

Key Words: Coronary artery disease; Follow-up studies; Hypercholesterolemia; Risk factors; Statin

Coronary heart disease (CHD) represents one of the main causes of death in the USA and Europe[1] and is the second most frequent cause of death in Japan.[2] CHD risk increases remarkably with the accumulation of risk factors.[3–5] Data from some epidemiological studies and clinical trials have identified several risk factors for CHD[6,7] and some risk prediction scores for CHD were developed using risk factor analysis from these data. The Framingham risk model is a typical one.[8] However, it is well known that the estimated incidence of CHD by the Framingham prediction model is not consistent with the actual incidence in different populations. Therefore, different prediction scores have been developed in several countries.[9–12] In 2006, the Health Risk Evaluation Chart,[13] a risk chart corresponding to the Framingham CHD risk score, was developed based on the Nippon Data 80,[14] which used a 19-year follow-up study of data of the Japanese general population.

(Received March 6, 2008; revised manuscript received May 29, 2008; accepted June 11, 2008; released online September 2, 2008)
*Department of Internal Medicine, Teikyo University School of Medicine, *Department of Biostatistics/Epidemiology and Preventive Health Sciences, The University of Tokyo, **Nakaya Clinic, Tokyo, †Biochemistry, Cell Biology and Metabolism, Nagoya City University Graduate School of Medical Sciences, Nagoya, ††Department of Medicine, Nippon Medical School and ‡Mitsukoshi Health and Welfare Foundation, Tokyo, Japan*
Mailing address: Tamio Teramoto, MD, Department of Internal Medicine, Teikyo University School of Medicine, 2-11-1 Kaga, Itabashi-ku, Tokyo 173-8605, Japan. E-mail: ttera@med.teikyo-u.ac.jp

Thus, despite the different risk prediction tools available in several countries, it remains unclear whether these tools accurately predict risk in patients with hypercholesterolemia treated by diet with or without a statin. Regarding risk prediction for the population receiving lipid-lowering pharmacotherapy, the CHD predicted value obtained from the Framingham risk model was compared with the observed CHD incidence in a substudy of WOSCOPS,[15] conducted to confirm the efficacy of pravastatin to prevent the first onset of ischemic heart disease. The observed incidence of CHD was similar to the predicted CHD risk using the Framingham risk model in the placebo group, whereas in the pravastatin group the observed CHD incidence was lower than the predicted CHD risk, indicating that the Framingham risk model does not accurately apply to patients receiving pravastatin.[16]

The MEGA study is a large-scale clinical study conducted to evaluate the efficacy of pravastatin treatment to decrease the risk of cardiovascular events in patients with mild to moderate hypercholesterolemia without a past history of ischemic heart disease and/or stroke.[17,18] This report shows that 2 different 5-year CHD incidence risk prediction tools, a risk prediction score and chart, developed from the MEGA study data is accurate and efficient for clinical application.

Methods

The MEGA study, a prospective randomized open-label study, was conducted from February 1994 to March 2004. A total of 8,214 patients with hypercholesterolemia (total cholesterol (TC) 220–270 mg/dl) and no history of ischemic

Table 1 Baseline Characteristics of Study Patients in the MEGA Study

	Diet group	*Diet plus pravastatin group*
No. of patients	*3,966*	*3,866*
Age (years)	*58.4±7.2*	*58.2±7.3*
Women	*2,718 (69%)*	*2,638 (68%)*
BMI (kg/m²)	*23.8±3.0*	*23.8±3.1*
SBP (mmHg)	*132.4±16.8*	*132.0±16.8*
DBP (mmHg)	*78.8±10.2*	*78.4±10.4*
*HT**	*1,664 (42%)*	*1,613 (42%)*
*Glucose abnormality***	*828 (21%)*	*804 (21%)*
Current/past smoker	*791 (20%)*	*823 (21%)*
TC (mg/dl)	*242.6±12.2*	*242.6±12.1*
TG (mg/dl)†	*127.5 (37.0–1,322.5)*	*127.4 (34.5–1,010.0)*
HDL-C (mg/dl)	*57.5±15.1*	*57.5±15.0*
LDL-C (mg/dl)	*156.5±17.6*	*156.6±17.5*
Lipoprotein(a) (mg/dl)	*24.7±25.2*	*24.7±25.6*

**Reported by physicians. **Documented diabetes and it also included the patients who had fasting glucose equal or greater than 110 mg/dl (impaired fasting glcose). †Data are median (interquartile range). All data are mean±SD or number (%) unless otherwise indicated.*

BMI, body mass index; SBP, systolic blood pressure; DBP, diastolic blood pressure; HT, hypertension; TC, total cholesterol; TG, triglyceride; HDL-C, high-density lipoprotein-cholesterol; LDL-C, low-density lipoprotein-cholesterol.

heart disease or stroke were enrolled. They comprised men of 40–70 years of age and post-menopausal women up to 70 years of age. The patients were assigned either to diet alone (diet group) or diet in combination with pravastatin treatment (10–20 mg/day, approved dose in Japan; diet plus pravastatin group). The mean follow-up period was 5.3 years. The primary endpoint was CHD (fatal and non-fatal myocardial infarction, angina pectoris, cardiac/sudden death, and angioplasty). Secondary endpoints were stroke, all cardiovascular disease, and total mortality. Major exclusion criteria included familial hypercholesterolemia, a history of cardiovascular disease, a current diagnosis of malignancy, and secondary hyperlipidemia.

Patients were evaluated, including the onset of endpoints, by the attending physician at 1, 3 and 6 months after the start of follow-up and every 6 months thereafter.

For each event, the diagnosis was made by the attending physician (including data from electrocardiogram and myocardial scintigraphy as needed) and reported in detail. Electrocardiography was performed annually. Information on individual patients was entered in the case report forms by their attending physicians and reported to the central Data Center. The Endpoint Committee evaluated each event in a blinded manner according to the criteria we reported previously.[17] Throughout the study period, TC, high-density lipoprotein-cholesterol (HDL-C), triglycerides (TG), and lipoprotein(a) [Lp(a)] concentrations were centrally measured at the same laboratory using methods standardized by the Centers for Disease Control and Prevention (CDC; Atlanta, GA). Low-density lipoprotein-cholesterol (LDL-C) concentration was estimated by the Friedewald formula.[19] The intention-to-treat analysis comprised 7,832 patients. Details of the design of MEGA study and the main results were reported previously.[17]

To construct the risk prediction tools, 7,760 of the 7,832 patients were evaluated using explanatory variables (72 of the 7,832 patients were excluded because of missing explanatory variables). To determine the explanatory variables, a univariate analysis was performed and then the significant factors were incorporated into the multivariate analysis model. For the risk factors determined by this multivariate model, $p<0.20$ served as the criterion for backward elimination of variables. The factors included in the tools were: treatment group (diet group, diet plus pravastatin group), sex (male, female), age (≤54, 55–59, 60–64, ≥65 years), baseline HDL-C (<40, 40–<60, ≥60 mg/dl), baseline LDL-C (<140, 140–<160, ≥160 mg/dl), glucose abnormality and hypertension (none, hypertension and normal fasting blood glucose concentration, glucose abnormality and normal blood pressure, glucose abnormality and hypertension), and smoking habit (non-smoker [including ex-smoker], smokers). Although baseline LDL-C was not identified as a risk factor for CHD in the present study, it was included in the MEGA risk tools because it was included in other risk prediction models. Because abnormality in glucose tolerance was included in glucose abnormality as a risk factor in the Guidelines for Arteriosclerosis 2007[20] patients with a fasting blood glucose concentration ≥110 mg/dl were included as diabetics in the present study.

To construct the MEGA risk prediction score, each risk score was established as an integer, taking into consideration the coefficient of each explanatory variable. The total risk score of each patient was calculated as a sum of the risk scores, and classified into 5 risk levels based on population quintiles for both treatment groups. The 5-year predicted value by each risk level was estimated from the Cox proportional hazard model to be used as the mean value of the predicted value at 5 years for each patient, and calculated for each treatment group.[21] To confirm the precision of the MEGA risk prediction model, we visually compared the estimated value to the observed value, and we plotted the receiver operating characteristic (ROC) curve using the development of CHD as the endpoint, and predictability was compared using the area under the ROC curve.

Further, we developed a simple, 5-year risk prediction chart based on the coefficient of each explanatory variable. The MEGA 5-year risk assessment chart for CHD displays the lipid parameters (HDL-C, LDL-C) by age on the y-axis and the characteristics associated with CHD risk (sex, smoking, hypertension, glucose abnormality) on the x-axis. In constructing the chart, the 2 categories of HDL-C (<40, 40–<60 mg/dl) and LDL-C (140–<160, ≥160 mg/dl) were integrated because the risk scores were set to the same degree. The 5-year CHD risk of each cell was estimated by the Cox proportional hazard model, and 8 levels of risk defined (each with its own color). The layout of the chart optimizes

Table 2 The β-Coefficients and HRs of the Multivariable Cox Proportional Hazard Model for 5-Year Risk of Coronary Heart Disease

	β	HR	95%CI
Groups			
Diet group	*0*	*1.00*	–
Diet plus pravastatin group	*−0.350*	*0.70*	*0.50–0.99*
Sex			
Women	*0*	*1.00*	–
Men	*0.784*	*2.19*	*1.49–3.21*
Age			
<55	*0*	*1.00*	–
55–59	*0.231*	*1.26*	*0.72–2.19*
60–64	*0.566*	*1.76*	*1.07–2.89*
≥65	*0.932*	*2.54*	*1.58–4.08*
HDL-C (mg/dl)			
≥60	*0*	*1.00*	–
40–<60	*0.714*	*2.04*	*1.29–3.24*
<40	*0.683*	*1.98*	*1.05–3.74*
LDL-C (mg/dl)			
<140	*0*	*1.00*	–
140–<160	*0.230*	*1.26*	*0.72–2.19*
≥160	*0.274*	*1.32*	*0.76–2.29*
HT, glucose abnormality***			
No	*0*	*1.00*	–
HT and normal fasting glucose†	*1.125*	*3.08*	*1.71–5.55*
Glucose abnormality and normal BP††	*1.646*	*5.19*	*2.88–9.35*
Glucose abnormality and HT	*1.992*	*7.33*	*4.12–13.04*
Current smoker			
No	*0*	*1.00*	–
Yes	*0.409*	*1.51*	*0.99–2.28*

**Documented. **Documented diabetes and it also included the patients who had fasting glucose equal or greater than 110 mg/dl (impaired fasting glcose). †Normal fasting glucose was defined as patients meet following criteria; reported as non-diabetes by physicians and fasting plasma glucose less than 110 mg/dl. ††Normal BP was defind as patients reported as non-HT by physicians. HR, hazard ratio; CI, confidence interval; BP, blood pressure. Other abbreviations see in Table 1.*

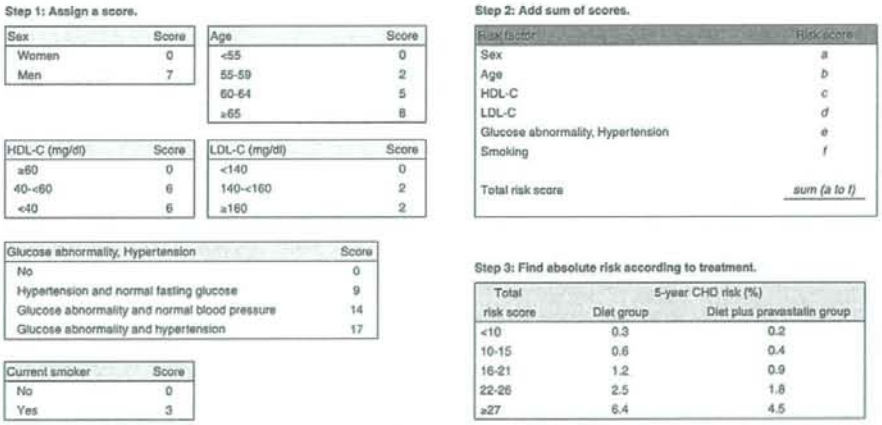

Fig 1. Simplified calculation form for estimating the 5-year risk of coronary heart disease (CHD) incidence in the diet group and diet plus pravastatin group. HDL-C, high-density lipoprotein-cholesterol: LDL-C, low-density lipoprotein-cholesterol.

the visual expression of the person's risk level from low to high with an 8-color gradation from the lower-left to the upper-right. For statistical analyses, the SAS software (release 8.2, SAS Institute, Cary, NC, USA) was used.

Results

During the 5-year follow-up, 138 CHD events were observed in the MEGA study. The baseline characteristics of the study population are shown in Table 1. The coefficient of each risk factor for CHD obtained from the Cox proportional hazard model and hazard ratio are shown in Table 2, and the 5-year risk prediction processes using the MEGA risk prediction score for CHD are summarized in Fig 1. A proportionally higher risk score was found for glucose abnormality alone (risk score 14), hypertension alone (risk

Table 3 Baseline Characteristics in Each Risk Level

	Total risk score				
	<10	10–<16	16–<22	22–<27	27–
Risk level	1	2	3	4	5
No. of patients	1,434	1,517	1,719	1,414	1,676
Age (years)	55.22±5.70	57.17±6.87	58.52±7.52	60.26±7.10	60.20±7.24
Women	1,336 (93.2%)	1,162 (76.6%)	1,238 (72.0%)	986 (69.7%)	607 (36.2%)
BMI (kg/m^2)	22.62±2.83	23.57±2.90	23.89±3.08	24.40±3.14	24.55±3.07
SBP (mmHg)	123.78±14.87	129.11±15.36	133.63±16.69	135.97±16.45	137.40±16.71
DBP (mmHg)	74.68±9.57	77.19±9.88	79.49±10.18	80.49±9.93	80.66±10.51
HT*	38 (2.6%)	320 (21.1%)	893 (51.9%)	961 (68.0%)	1,033 (61.6%)
Glucose abnormality**	0 (0.0%)	19 (1.3%)	251 (14.6%)	516 (36.5%)	1,395 (83.2%)
Current smoker	38 (2.6%)	123 (8.1%)	333 (19.4%)	156 (11.0%)	511 (30.5%)
TC (mg/dl)	242.80±12.30	242.69±11.86	243.62±12.00	241.97±12.03	241.78±12.14
LDL-C (mg/dl)	151.04±17.81	157.33±17.40	157.39±16.89	157.50±17.23	159.21±17.16
HDL-C (mg/dl)	69.77±14.45	58.57±14.01	58.06±14.52	53.56±12.86	49.44±10.59
TG (mg/dl)†	98.5 (37.5–519.0)	120.3 (37.0–675.7)	126.0 (34.5–656.0)	142.3 (42.0–486.5)	152.7 (43.0–775.0)
Lipoprotein(a) (mg/dl)	27.03±27.82	25.76±26.85	25.02±25.53	24.33±24.83	22.16±22.75

*Reported by physicians. **Documented diabetes and it also included the patients who had fasting glucose equal or greater than 110 mg/dl (impaired fasting glucose). †Data are median (interquartile range). All data are mean±SD or number (%) unless otherwise indicated. The 72 patients were excluded from this analysis because of missing data of the risk factors for coronary heart disease.

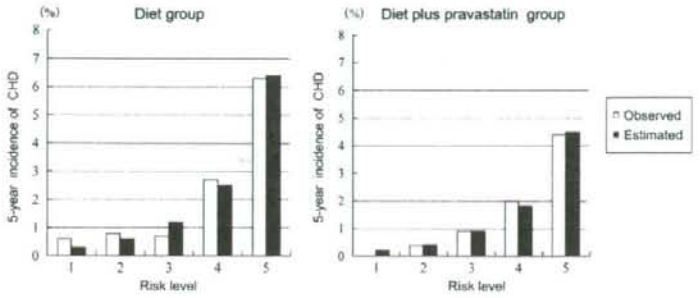

Fig 2. Comparison between the observed and estimated 5-year incidence of coronary heart disease (CHD) for the diet group and the diet plus pravastatin group.

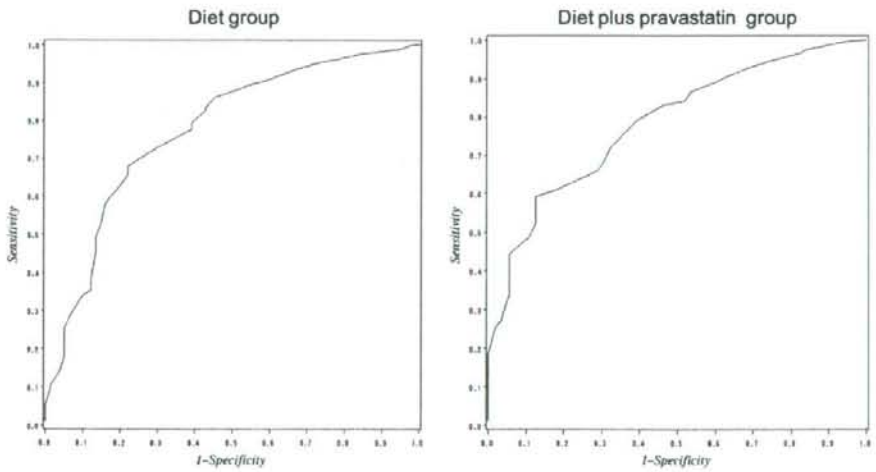

Fig 3. Receiver operating characteristic curves for the diet group and diet plus pravastatin group.

score 9) and their combination (risk score 17) compared to the scores for men (risk score 7), age ≥65 years (risk score 8), and low HDL-C (risk score 6).

Notably, the risk scores for a high LDL-C (risk score 2) and smoking (risk score 3) were lower than those for the other risk factors. The risk quintiles were determined by the intrinsic cut-off points of 10, 16, 22 and 27.

Table 3 shows patients' background factors as classified by risk level. Mean age tended to be higher for the higher risk levels. There were more women than men in the lower

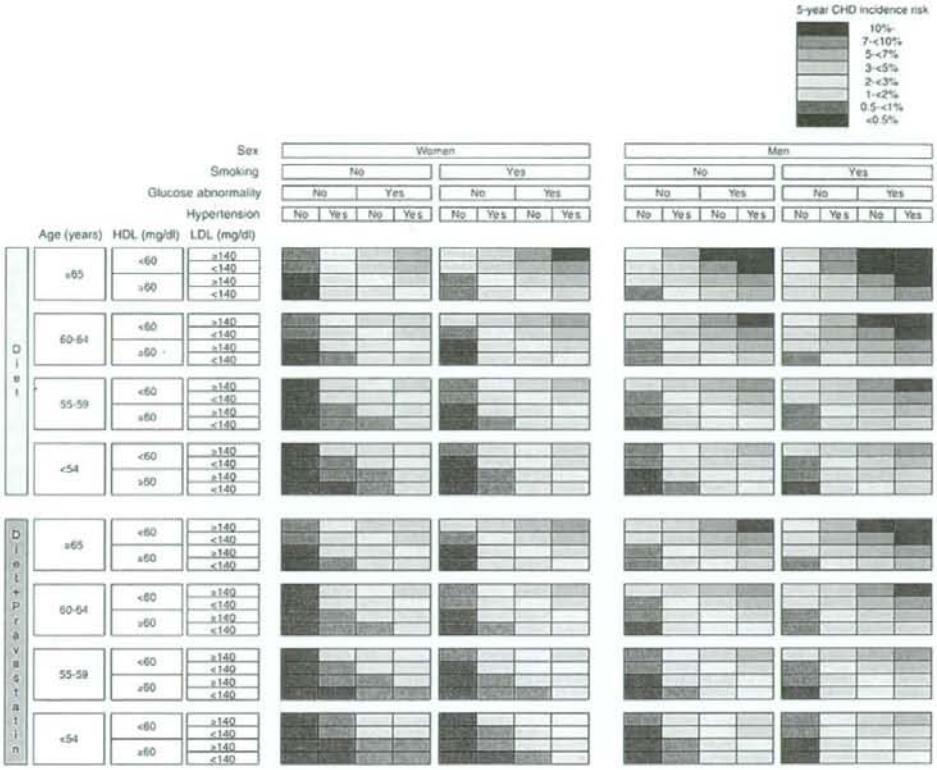

Fig 4. Risk assessment chart for 5-year risk of coronary heart disease (CHD) incidence, including sex, age, high-density lipoprotein (HDL)-cholesterol, low-density lipoprotein (LDL)-cholesterol, glucose abnormality (including impaired fasting glucose), hypertension, and smoking.

risk levels. Body mass index increased (ranging from 0.26 to 0.91) for each increase of 1 risk level. Prevalence of glucose abnormality (documented diabetes and high fasting blood sugar concentration), hypertension, and smoking habit were greater in the higher risk levels, whereas TC concentration was similar across risk levels. LDL-C concentrations were similar for the 4 highest levels of risk and were somewhat lower for the lowest risk level. HDL-C concentrations were higher at the lower levels of risk and tended to decrease as the level of risk increased. TG tended to increase slightly as the risk levels increased, whereas concentrations of Lp(a) tended to decrease slightly as the risk levels increased.

The specificity of the MEGA risk assessment was validated with good concordance between the 5-year predicted values and the observed incidence. The range of the 5-year predicted values was similar for the predicted values (ranging from 0.3% to 6.4% diet group, 0.2% to 4.5% diet plus pravastatin group) and the observed values (0.6% to 6.3% diet group, 0 to 4.4% diet plus pravastatin group, Fig 2). The area under the curve (AUC) for the ROC curves was 0.774 for the diet group and 0.784 for the diet plus pravastatin group (Fig 3).

The MEGA risk prediction chart was constructed as shown in Fig 4. It depicts the increasing risk with its 8-color grading, according to the combination of risk factors in men and women in each treatment group. The 5-year predicted risk was higher in the diet group than in the diet plus pravastatin group. A 5-year CHD risk ≥10% was found for men >65 years old and men 60–64 years old who were smokers and diabetic in the diet group (red cells), and for women >65 years old who were smokers and had glucose abnormality plus hypertension. When all the risk factors were present, the highest predicted risk was estimated at 21% for men and at 10% for women <65 years old in the diet group (data not shown).

Discussion

The MEGA risk prediction score and MEGA risk prediction chart reported here are CHD risk assessment tools developed using MEGA study data. The MEGA risk score easily predicts 5 grades of 5-year CHD risk, and even greater accuracy of risk prediction is achieved with the MEGA risk chart with 8 grades of risk, in mild to moderate hypercholesterolemia without a history of cardiovascular disease. The risk factors included in the MEGA risk prediction tools have been well known as CHD risk factors[6,7,22] The accumulation of these risk factors is associated with a higher CHD risk[14] and the MEGA risk tools are consistent with these findings.

The MEGA Study included patients with hypercholester-

olemia who were 40 to 70 years old (postmenopausal women <70 years) with a TC concentration of 220–270 mg/dl and no past history of cardiovascular disease. These patients were recruited from outpatient clinics, therefore, the MEGA risk tools are useful to predict the likelihood of developing CHD over 5 years in typical people with mild to moderate hypercholesterolemia with no history of cardiovascular disease. A key characteristic of the MEGA risk tools is that it is possible to assess risk in people treated with diet alone and in people receiving pharmacotherapy. Notably, the Framingham risk score did not predict risk accurately in patients treated with pravastatin in a WOSCOPS substudy.[16]

Interestingly, an exponential increase in the predicted value was found as the risk levels increased. A near doubling in the 5-year predicted value from risk level 1 to risk level 2 was found with the MEGA risk prediction score. An even greater increase in predicted value was seen when risk was increased from level 4 to level 5.

Notably, little difference was seen between the estimated and observed incidence of CHD in both treatment groups with the MEGA risk score. This is consistent with what would be expected, when considering the association between the distribution of cases with risk factors and the increasing CHD risk across risk levels (Table 2).

The AUC of the ROC curve plotted in terms of total risk score for each treatment group was higher than 0.77 in both treatment groups. In a study reported previously, the AUC was 0.76 for the prediction of the main cardiovascular events (fatal and non-fatal myocardial infarction, coronary insufficiency [prolonged angina with documented electrocardiographic changes], heart failure, and stroke) using the Framingham risk model.[3] Thus, the correspondence between these AUC values indicate the CHD risk predicted by the MEGA risk prediction score has a precision similar to that by the Framingham risk model.

A lower 5-year predicted risk was obtained with the MEGA risk prediction score than with the Framingham risk model. For the diet only treatment group, the predicted risk was one-sixth lower in the low-risk level and two-thirds lower in the high-risk level with the MEGA risk score compared with the Framingham model. A simple comparison of the 2 prediction models might not be possible because the Framingham model was developed based on a general population without left ventricular hypertrophy (LVH), whereas the MEGA Study included patients with LVH. Further, it has been reported that the Framingham risk model is not applicable in different populations.[24,25] Thus, the MEGA risk score might be superior in its accuracy for determining CHD risk in patients with moderate hypercholesterolemia, such as Japanese patients.

The MEGA risk prediction chart provides even greater accuracy because of the incorporation of multiple risk factors. The 8 levels of risk predicted are color-coded, with the 5-year risk increasing from the bottom-left to upper-right of the chart, according to sex and age in combination with lipid factors and smoking, glucose abnormality, and hypertension. Concordance between the MEGA risk score and the MEGA risk chart is validated by the use of the same analysis model for both, with a different β coefficiency used for the risk chart to account for it having 1 less category of HDL-C and LDL-C than the risk score.

In the present study, 2 types of risk prediction tools were developed that apply to each treatment group. As noted previously, the Framingham risk model has been shown to underestimate the risk in patients who are treated with a statin. A substudy of WOSCOPS, a primary prevention study similar to our study, calculated CHD risk using the Framingham risk model and compared the observed incidence using time course changes in mean concentrations of serum cholesterol and HDL-C.[15] In the placebo group the observed incidence and predicted risk were similar, whereas in the pravastatin group the observed incidence was lower than the predicted risk. Thus, the efficacy of pravastatin to reduce CHD risk is not sufficiently explained by changes in serum lipid concentrations, based on the Framingham risk model. It seems, therefore, that CHD risk should be calculated separately based on treatment or not with a statin.

There are a few limitations to our analyses. First, the MEGA risk prediction tools are applicable to patients with mild to moderate hypercholesterolemia (TC 220–270 mg/dl). Notably, however, 70% of the estimated 20 million ambulatory patients with hypercholesterolemia in Japan fall within this range. Second, the MEGA prediction tools are applicable to treated patients only, including diet treatment, as it is based on data from patients treated in the MEGA study. The predicted CHD risk for untreated persons using the MEGA risk tools is likely to be lower than the actual risk. Third, these risk prediction tools are based on data in Japanese patients, although it is feasible to consider using these tools in people with a similar profile.

We believe the MEGA risk prediction tools are valuable for use in usual clinical practice, with greater ease and accuracy to predict the 5-year CHD risk in patients with mild to moderate hypercholesterolemic patients, such as Japanese patients. Moreover, these are highly useful as educational tools for high-risk patients.

Acknowledgment

This study was financially supported by the Japanese Ministry of Health, Labor and Welfare for the first 2 years of the study, and thereafter the study was funded by Daiichi-Sankyo Co, Ltd, Tokyo, Japan.

References

1. American Heart Association. Heart disease and stroke statistics: 2006 update. Dallas: American Heart Association, 2006.
2. Health and Welfare Statistics Association. Statistical Abstracts on Health and Welfare in Japan 2006. Tokyo: Health and Welfare Statistics Association, 2007.
3. Kannel WB, Dawber TR, Kagen A, Revotskie N, Stokes J 3rd. Factors of risk in the development of coronary heart disease–six year follow-up experience: The Framingham Study. *Ann Intern Med* 1961; **55:** 33–50.
4. Satoh H, Nishino T, Tomita K, Saijo Y, Kishi R, Tsutsui H. Risk factors and the incidence of coronary artery disease in young middle-aged Japanese men: Results from a 10-year cohort study. *Intern Med* 2006; **45:** 235–239.
5. Okamura T, Nakamura K, Kanda H, Hayakawa T, Hozawa A, Murakami Y, et al; Health Promotion Research Committee, Shiga National Health Insurance Organizations. Effect of combined cardiovascular risk factors on individual and population medical expenditures: A 10-year cohort study of national health insurance in a Japanese population. *Circ J* 2007; **71:** 807–813.
6. Jousilahti P, Vartiainen E, Tuomilehto J, Puska P. Sex, age, cardiovascular risk factors, and coronary heart disease: A prospective follow-up study of 14 786 middle-aged men and women in Finland. *Circulation* 1999; **99:** 1165–1172.
7. The West of Scotland Coronary Prevention Study Group, Cobbe SM. Baseline risk factors and their association with butcome in the West of Scotland Coronary Prevention Study: The West of Scotland Coronary Prevention Study Group. *Am J Cardiol* 1997; **79:** 756–762.
8. Wilson PW, D'Agostino RB, Levy D, Belanger AM, Silbershatz H, Kannel WB. Prediction of coronary heart disease using risk factor categories. *Circulation* 1998; **97:** 1837–1847.
9. Knuiman MW, Vu HT. Prediction of coronary heart disease mortality in Busselton, Western Australia: An evaluation of the Framingham

national health epidemiologic follow up study, and WHO ERICA risk scores. *J Epidemiol Community Health* 1997; **51:** 515–519.
10. Thomsen TF, Davidsen M, Ibsen H, Jorgensen T, Jensen G, Borch-Johnsen K. A new method for CHD prediction and prevention based on regional risk scores and randomized clinical trials; PRECARD and the Copenhagen Risk Score. *J Cardiovasc Risk* 2001; **8:** 291–297.
11. Conroy RM, Pyorala K, Fitzgerald AP, Sans S, Menotti A, De Backer G, et al. Estimation of ten-year risk of fatal cardiovascular disease in Europe: The SCORE project. *Eur Heart J* 2003; **24:** 987–1003.
12. Hippisley-Cox J, Coupland C, Vinogradova Y, Robson J, May M, Brindle P. Derivation and validation of QRISK, a new cardiovascular disease risk score for the United Kingdom: Prospective open cohort study. *BMJ* 2007; **335:** 136–141.
13. NIPPON DATA80 Research Group. Risk assessment chart for death from cardiovascular disease based on a 19-year follow-up study of a Japanese representative population. *Circ J* 2006; **70:** 1249–1255.
14. Nakamura Y, Yamamoto T, Okamura T, Kadowaki T, Hayakawa T, Kita Y, et al; The NIPPON DATA 80 Research Group. Combined cardiovascular risk factors and outcome: NIPPON DATA80, 1980–1994. *Circ J* 2006; **70:** 960–964.
15. Shepherd J, Cobbe SM, Ford I, Isles CG, Lorimer AR, MacFarlane PW, et al. Prevention of coronary heart disease with pravastatin in men with hypercholesterolemia. *N Engl J Med* 1995; **333:** 1301–1307.
16. West of Scotland Coronary Prevention Study Group. Influence of pravastatin and plasma lipids on clinical events in the West of Scotland Coronary Prevention Study (WOSCOPS). *Circulation* 1998; **97:** 1440–1445.
17. Management of Elevated Cholesterol in the Primary Prevention Group of Adult Japanese (MEGA) Study Group. Design and baseline characteristics of a study of primary prevention of coronary events with pravastatin among Japanese with mildly elevated cholesterol levels. *Circ J* 2004; **68:** 860–867.
18. Nakamura H, Arakawa K, Itakura H, Kitabatake A, Goto Y, Toyota T, et al; MEGA Study Group. Primary prevention of cardiovascular disease in Japan: Results of the management of elevated cholesterol in the primary prevention group of adult Japanese (MEGA), randomised study with pravastatin. *Lancet* 2006; **368:** 1155–1163.
19. Friedewald WT, Levy RI, Fredrickson DS. Estimation of the concentration of low-density lipoprotein cholesterol in plasma, without use of the preparative ultracentrifuge. *Clin Chem* 1972; **18:** 499–502.
20. Teramoto T, Sasaki J, Ueshima H, Egusa G, Kinoshita M, Shimamoto K, et al. Executive Summary of Japan Atherosclerosis Society (JAS) Guideline for Diagnosis and Prevention of Atherosclerotic Cardiovascular Diseases for Japanese. *J Atheroscler Thromb* 2007; **14:** 45–50.
21. Kalbfleisch JD, Prentice RL. The statistical analysis of failure time data, 2nd edn. New York: John Wiley & Sons; 2002.
22. Yamamoto A, Richie G, Nakamura H, Hosoda S, Nobuyoshi M, Matsuzaki M, et al; ASPAC study members in Japan; Research Committee on Serum Lipid Survey 1990 Japan. Risk factors for coronary heart disease in the Japanese–comparison of the background of patients with acute coronary syndrome in the ASPAC study with data obtained from the general population: Asia-Pacific Collaboration on CHD Risk Factor Intervention study. *J Atheroscler Thromb* 2002; **9:** 191–199.
23. Wang TJ, Gona P, Larson MG, Tofler GH, Levy D, Newton-Cheh C, et al. Multiple biomarkers for the prediction of first major cardiovascular events and death. *N Engl J Med* 2006; **355:** 2631–2639.
24. de Visser CL, Bilo HJ, Thomsen TF, Groenier KH, Meyboom-de Jong B. Prediction of coronary heart disease: A comparison between the Copenhagen risk score and the Framingham risk score applied to a Dutch population. *J Intern Med* 2003; **253:** 553–562.
25. Neuhauser HK, Ellert U, Kurth BM. A comparison of Framingham and SCORE-based cardiovascular risk estimates in participants of the German National Health Interview and Examination Survey 1998. *Eur J Cardiovasc Prev Rehabil* 2005; **12:** 442–450.

Involvement of Protein Kinase D in Phosphorylation and Increase of DNA Binding of Activator Protein 2α to Downregulate ATP-Binding Cassette Transporter A1

Noriyuki Iwamoto, Sumiko Abe-Dohmae, Rui Lu, Shinji Yokoyama

Background—Activator protein (AP) 2α negatively regulates expression of ABCA1 gene through Ser-phosphorylation of AP2α (*Circ Res.* 2007;101:156–165). Potential specific Ser-phosphorylation sites for this reaction were investigated in human AP2α.

Methods and Results—The phosphorylation was shown mediated by PKD, and Ser258 and Ser326 were found in its specific phosphorylation sequence segment in AP2α. PKD phosphorylated Ser258 more than Ser326 and induced its binding to the ABCA1 promoter. These reactions and AP2α-induced suppression of the ABCA1 promoter activity were reversed by mutation of Ser258 more than Ser326 mutation. Knockdown of PKD by siRNA reduced the AP2α Ser-phosphorylation, and increased ABCA1 expression and HDL biogenesis. Gö6983 inhibited PKD more selectively than PKC in THP-1 and HEK 293 cells and in mice, and increased ABCA1 expression, HDL biogenesis, and plasma HDL level.

Conclusion—PKD phosphorylates AP2α to negatively regulate expression of ABCA1 gene to increase HDL biogenesis. The major functional phosphorylation of AP2α was identified at Ser258 by PKD, in the AP2α basic domain highly conserved among species and all 5 subtypes of AP2. PKD/AP2 system can be a potent pharmacological target for prevention of atherosclerosis. **(*Arterioscler Thromb Vasc Biol.* 2008;28:2282-2287.)**

Key Words: HDL ■ ABCA1 ■ AP2α ■ PKD ■ doxazosin ■ atherosclerosis

We recently reported that activator protein (AP) 2α negatively regulates expression of the ATP-binding cassette transporter (ABC) A1 gene, and inhibition of this system accordingly increases ABCA1 and high-density lipoprotein (HDL) biogenesis.[1] We proposed that serine (Ser)-phosphorylation of AP2α is a candidate for a regulatory mechanism for its interaction with the ABCA1 promoter.

As illustrated in supplemental Figure I (available online at http://atvb.ahajournals.org), AP2α is reportedly phosphorylated by protein kinase A (PKA) at Ser239 in its basic domain for transactivation of the apolipoprotein (apo) E promoter, but its mutation to alanine (Ala) to abolish this phosphorylation did not influence the AP2α binding to the apoE promoter.[2] Therefore, the Ser-phosphorylation of AP2α to regulate its DNA binding should take place at other residue(s) than this. In addition to Ser239 in a PKA-phosphorylation motif RRXS/T (supplemental Figure IB),[2] Ser258 and Ser326 were found consisting a segment LXRXXS/T, a phosphorylation motif by protein kinase D (PKD).[3] There is no additional potential site for PKD-mediated phosphorylation and no potential Ser-phosphorylation site for protein kinase C (PKC) (K/R X S/T X K/R).

The central basic domain and the helix-span-helix motif mediate DNA binding of AP2α.[4,5] These domains mediate forming hetero- and homo-dimers of AP2, and this dimerization is required for the DNA binding activity. The proline- and glutamine-rich domain at the N terminus is responsible for transactivation. Therefore, the functional phosphorylation site may be located in this region. Referring to supplemental Figure I, Ser258 is in the basic domain conserved among species, and all 5 subtypes of AP2α, β, δ, γ, and ε and Ser326 was also found conserved in the helix-span-helix motif, corresponding to 247 and 315 in xenopus AP2α that are also in a PKD phosphorylation motif.[4,5] Interestingly, the LXRXXS (Ser277) motif of the AP2β basic domain is completely identical to that of AP2α, and AP2β was shown to directly bind to the adiponectin promoter and inhibit its transcriptional activity.[6] Therefore, it would be rational to hypothesize that PKD is involved in regulation of the AP2-mediated gene expression.

PKD is a Ser/threonine (Thr) kinase,[7,8] activated by cell-growth promoting reagents such as phorbol 12-myristate 13-acetate (PMA), platelet derived growth factor (PDGF), and G protein–coupled receptor (GPCR) ligands.[9–12] It seems related to cell proliferation, as overexpression of PKD increases DNA synthesis and cell growth,[13] and stimulates the Raf-MEK-extracellular signal regulated kinase (ERK) path-

Original received July 25, 2008; final version accepted September 29, 2008.

From Biochemistry, Nagoya City University Graduate School of Medical Sciences, Nagoya, Japan.

Correspondence to Dr Shinji Yokoyama, Biochemistry, Nagoya City University Graduate School of Medical Sciences, Kawasumi 1, Mizuho-cho, Mizuho-ku, Nagoya 467-8601, Japan. E-mail syokoyam@med.nagoya-cu.ac.jp

Arterioscler Thromb Vasc Biol **is available at http://atvb.ahajournals.org** **DOI: 10.1161/ATVBAHA.108.174714**

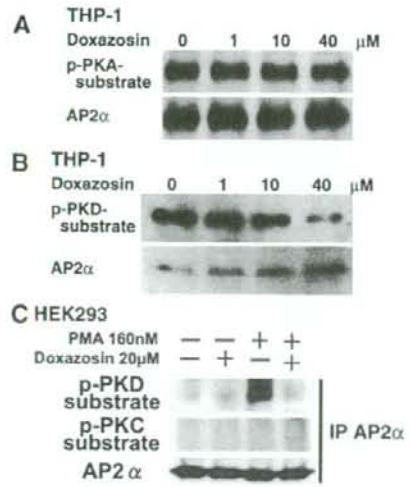

Figure 1. Phosphorylation of AP2α by PKD. Effect of doxazsoin on AP2α phosphorylation mediated by PKA (A) and PKD (B) in THP-1 macrophage. The immunoprecipitated protein by anti-AP2α antibody was analyzed by Western blotting by using antibodies against phospho-specific substrates of PKA and PKD. C, Inhibition of PKD-mediated phosphorylation of AP2α by doxazosin. AP2α expression vector was transfected and expressed in HEK293 cells. Cells were incubated with PMA to induce phosphorylation in the presence and absence of doxazosin for 16 hours. The harvested cell proteins were analyzed as described above and also with antiphospho PKC substrate antibody.

way through the RIN1 phosphorylation.[14] AP2α is also associated with cell proliferation and differentiation. AP2α-deficient fibroblasts grow slower than the wild type.[15] AP2α level decreases in some carcinoma cells.[5,16,17] AP2α positively regulates the proto-oncogene c-erb-B2 expression.[18] Both PKD and AP2α could thus be related to the gene expression to regulate cellular growth and proliferation, and therefore PKD-mediated Ser-phosphorylation is a good candidate mechanism for regulation of this system.

In this study, we intended to identify the functional Ser-phosphorylation site of AP2α and to examine whether modulation of this system influences HDL metabolism hoping that AP2 signaling would be a new target for prevention of atherosclerosis.

Materials and Methods

Monoclonal antibody against human and mouse ABCA1 (MABI98-7)[19] was generated in rats at MAB Institute (Yokohama, Japan) by using a peptide CNFAKDQSDDDHLKDLSLHKN representing the amino acid sequence of the C terminus of human and mouse ABCA1. Apolipoprotein A-I (apoA-I) was isolated from human plasma HDL.[20] For luciferase reporter gene assay, ABCA1 promoter constructs were generated by polymerase chain reaction (PCR).[1] The plasmid for expression of pSG-neo-AP2α and the control vector[21] were kindly provided by Dr M. A. Tainsky (Wayne State University, Detroit, Mich). To introduce mutation of Ser to Ala into AP2α protein at the residues 258 or 326, site-directed mutation was introduced by using a Quick Change II Site-Directed Mutagenesis kit (Stratagene). Other general experimental procedures are available in the online supplemental materials.

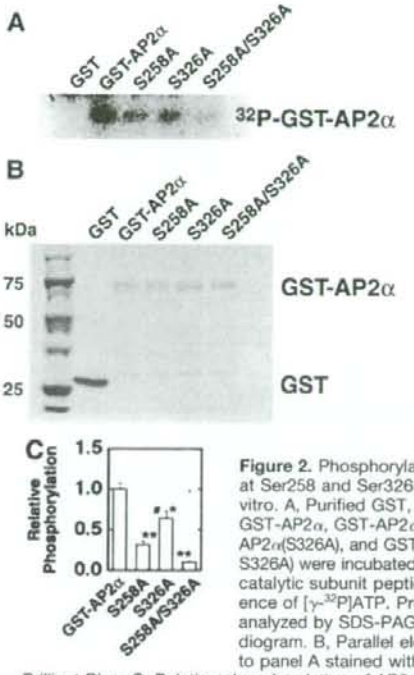

Figure 2. Phosphorylation of AP2α at Ser258 and Ser326 by PKD in vitro. A, Purified GST, wild-type GST-AP2α, GST-AP2α(S258A), GST-AP2α(S326A), and GST-AP2α(S258A/S326A) were incubated with the PKD catalytic subunit peptide in the presence of [γ-^{32}P]ATP. Proteins were analyzed by SDS-PAGE and autoradiogram. B, Parallel electrophoresis to panel A stained with Coomassie-Brilliant Blue. C, Relative phosphorylation of AP2α and its mutants, quantified from the results in A and B expressed as relative values to the GST-AP2α. * and ** indicate $P<0.05$ and 0.01, respectively, from the control GST-APα and # indicates $P<0.05$ from GST-AP2α(S258A). The data represent average±SD for 3 measurements.

Results

Phosphorylation of AP2α by PKD Regulates Its Binding to ABCA1 Promoter

Doxazosin that upregulated apoA-I–mediated cellular lipid release and increased mouse plasma HDL[1] did not influence AP2α phosphorylation at the PKA-specific site (Figure 1A). On the other hand, it reduced AP2α phosphorylation by PKD in dose-dependent fashion (Figure 1B). PMA increased AP2α phosphorylation by PKD but not that by PKC and doxazosin inhibited this action of PMA in HEK293 cells AP2α was transfected to (Figure 1C). Thus, phoshorylation of AP2α at a PKD-specific site(s) is involved in the doxazosin-related reactions.

Mutation to Ala was introduced at either or both of PKD phosphorylation sites of Ser258 and Ser326 in the glutathione S-transferase (GST)-AP2α fusion protein (Figure 2A). Wild-type GST-AP2α and GST-AP2α(S326A) proteins were phosphorylated by PKD. Phosphorylation of GST-AP2α(S258A) was less and phosphorylation of GST-AP2α(S258/326A) was undetectable (Figure 2B). The results showed that Ser258 is more efficiently phosphorylated by PKD.

DNA binding activity of the AP2α mutants was examined. The antibody equally recognizes both AP2α and AP2α(S258A) in HEK 293 cells (data not shown). As shown in Figure 3A by gel shift assay, PKD reaction increased the DNA binding of wild-type AP2α but not AP2α(S258A).

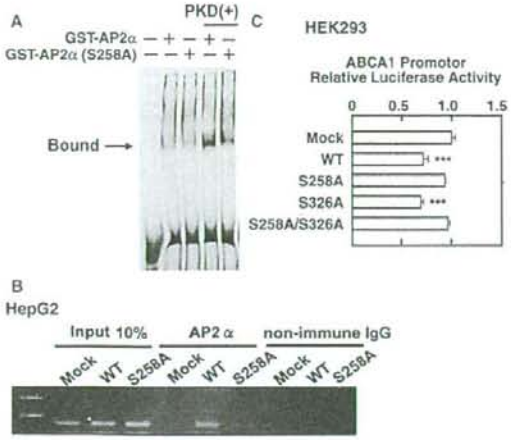

Figure 3. PKD phosphorylates AP2α Ser258 to increase DNA binding and suppress ABCA1 promoter activity. A, Gel shift assay for the AP2-binding site in the ABCA1 promoter for AP2α and AP2α(S258A) proteins in the presence and absence of the PKD catalytic subunit. B, ChIP assay for DNA binding. HepG2 cells that lack endogenous AP2α were transfected with AP2α and AP2α(S258A). Nuclear proteins cross-linked with DNA were immunoprecipitated by ant-AP2α antibody and PCR was performed for the AP2 binding site. C, ABCA1 promoter activity assay. ABCA1 promoter construct (WT-Luc) and AP2α were transfected to HEK293 cells. Luciferase activity was normalized for phRL-TK. *** indicates difference with $P<0.001$ from mock.

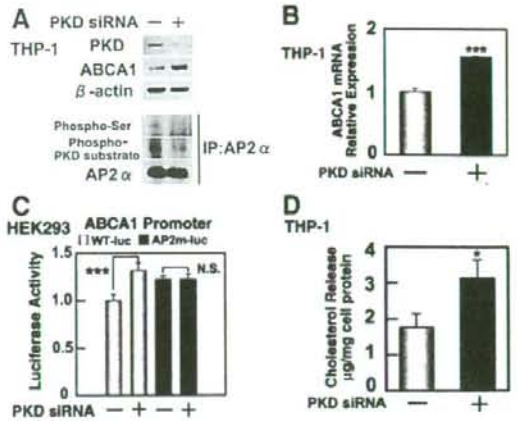

Figure 4. PKD-knockdown and ABCA1 expression/HDL biogenesis. A, PKD was knocked-down in THP-1 macrophages by siRNA, and cell protein (50 μg) was analyzed by Western blotting. Immunoprecipitatant with anti-AP2α antibody was analyzed by antiphospho-PKD substrate antibody. B, THP-1 cells were similarly treated and ABCA1 mRNA was analyzed. C, Activity of ABCA1 reporter construct of wild-type (WT-luc) and its AP2 binding site mutant (AP2m-luc) was measured in HEK293 cells with PKD-knockdown. D, THP-1 macrophages treated as above were incubated with apoA-I, and cholesterol release was measured. Data represent average±SD for triplicate assays. *$P<0.05$, **$P<0.01$, ***$P<0.001$ against scramble controls.

Chromatin immunoprecipitation (ChIP) analysis also demonstrated tight interaction of wild-type AP2α but not that of AP2α(S258A), which were transfected to HepG2 cells which lack endogenous AP2α,[22] together with the ABCA1 promoter containing the AP2 binding site (Figure 3B). Figure 3C shows inhibitory effect of AP2α and its mutants AP2α(S258A), AP2α(S326A), and AP2α(S258A/S326A) on the ABCA1 promoter activity. The inhibition by AP2α was reduced by mutation at Ser258. The results confirmed that phosphorylation of AP2α at Ser258 is essential for its binding to DNA and regulating the transcriptional activity.

Regulation by PKD of ABCA1 Activity and Other AP2-Regulated Genes

The small interfering (si) RNA treatment significantly reduced the PKD protein level and increased ABCA1 protein expression in THP-1 macrophage. It did not influence expression of AP2α, but its phosphorylation by PKD was strongly inhibited (Figure 4A). ABCA1 mRNA expression was also significantly increased by knockdown of PKD (Figure 4B). ABCA1 promoter activity was also upregulated by PKD-siRNA for the wild-type promoter in HEK293. Increase of the transcription activity was more prominent (by 100%) with the promoter of −369 to +110 (data not shown). On the other hand, its basic activity was increased, and the effect of siRNA was negative when the AP2 binding site of the promoter was mutated (Figure 4C). Knockdown of PKD increased the apoA-I–mediated free cholesterol release from THP-1 macrophage (Figure 4D). The results thus demonstrated that PKD inhibition decreased the AP2α activity for DNA binding, increased ABCA1 expression and enhanced the HDL biogenesis.

Effects of Protein Kinase Inhibitors on PKD in Cells and In Vivo

Doxazosin inhibited PKD-mediated AP2α phosphorylation in the mouse liver (Figure 5A), so that inhibition of PKD in vivo was attempted in mouse. Specific inhibitors for PKD are currently unavailable. PKD is activated through PKC-mediated phosphorylation of Ser744 and Ser748,[23–25] so that PKC inhibitors such as Gö6983, Gö6976, rottlerin, and doxazosin were tested for modulation of the PKD phosphorylation. Gö6983 most strongly and selectively inhibited PKD, whereas others did only moderately to generate consistent results with those by PKD siRNA, so that this compound was chosen for the in vivo study (these data are provided in supplemental Figures II and III). Gö6983 inhibited phosphorylation of PKD and AP-2α in the liver in mice, but not phosphorylation of proteins that were identified by using an antiphospho-PKC-substrate antibody (Figure 5B, 5C, and 5D). Gö6983 inhibited expression of SREBP1 in the liver, whereas it had no effect on SREBP2 in the liver and SREBP1 in the adipose tissue (Figure 5E).

Finally, we investigated whether PKD inhibition increases expression of the ABCA1 gene in vivo and thus leads to raising HDL level in plasma. As shown in Figure 6A, the mRNA and protein levels of ABCA1 were both increased in the liver by the Gö6983 treatment. High-performance liquid chromatography (HPLC) analysis of plasma demonstrated significant increase of HDL (Figure 6B and supplemental Table). Gö6983 also decreased plasma triglyceride, being consistent with the decrease of SREBP1 expression.